Preparation of ^{99m}Tc-PQQE and preliminary biological evaluation for the NMDA receptor

ZHOU Xingqin* KONG Yanyan ZOU Meifen
ZHANG Jiankang CAO Guoxian

Key Laboratory of Nuclear Medicine, Ministry of Health, Jiangsu Key Laboratory of Molecular Nuclear Medicine, Jiangsu Institute of Nuclear Medicine, Wuxi 214063, China

Abstract The 4,5-dioxo-4,5-dihydro-1H-pyrrolo(2,3-f)quinoline-2,7,9-tricarboxylic acid 2-ethyl ester 7,9-dimethyl ester (PQQE) was synthesized on the basis of Pyrroloquinoline quinine (PQQ). ^{99m}Tc-PQQE was prepared using stannous fluoride (SnF_2) as reducing agent. Biological characteristics of ^{99m}Tc-PQQE include lipophilic and the charge properties were compared to ^{99m}Tc-PQQ. The biodistributions of ^{99m}Tc-PQQE in mice and brain regional distribution were performed. *In vivo* distribution of ^{99m}Tc-PQQE in mice indicates that the concentration ratio of drug and blood increases steadily over time. The major radioactivity may be metabolized by the hepatic and renal system. The elimination-phase half-time (t1/2 β) results indicate that the residence time of ^{99m}Tc-PQQE (203.92) in the body is twice as long as ^{99m}Tc-PQQ (100.45). The uptake of ^{99m}Tc-PQQE in brain was improved due to the ameliorating of charge and lipophilicity. The highest total regional brain uptake of ^{99m}Tc-PQQE was in the frontal lobe and hippocampus, where the NMDA receptor is very abundant. ^{99m}Tc-PQQE had a good target to nontarget ratio (hippocampus/cerebellum) which preserved a higher value (peak 4.0 at 120 min) from 60 min to 180 min after injection. In vitro autoradiographic results are in close agreement with the regional brain map. The enrichment can be blocked by *N*-methyl-D-aspartate receptor (NMDAR) redox modulatory site antagonists-ebselen (EB). This work suggests that ^{99m}Tc-PQQE has some specific targeting to the NMDA receptor.

Key words PQQE, ^{99m}Tc-PQQE, NMDA receptor, Bodistribution, *in vitro* autoradiography assay

1 Introduction

Previous studies reported that electron-rich aromatic and poly-anionic compounds are the potential drugs for the mental because they can inhibit the replication of protein PrP-res[1,2]. Representative compounds are anthracene helix (co-conjugate quinone) and Congo red (poly-anionic).

Pyrroloquinoline quinine (PQQ, 4,5-dihydro-4,5-dioxo-1H-pyrrolo [2,3-f] quinoline-2,7,9-tricarboxylic acid) is a redox cofactor and is found in plants and animal tissues[3-6]. It also has very similar functional groups (conjugated quinone and anions) with the two types of compounds. It is an aromatic heterocyclic anionic orthoquinone that can readily react with different functional groups, such as amino acids, alcohols, and nucleophiles[7,8].

Recently, PQQ and its derivative have received attention for their ability to inhibit amyloid fibril formation[9], to protect the brain against oxidative damage[10,11]. Moreover, in human fibroblast cultures, PQQ and imidazolopyrroloquinoline, a derivative of PQQ, enhance cell growth and proliferation when added to cultures at nmol/L concentrations[12].

In the brain, *N*-methyl-D-aspartate receptor (NMDAR) is considered to be among the most critical molecular regulators of cognition, memory, motor control and synaptic plasticity. As an electron donor or NMDAR redox reaction site, PQQ readily reacts with nucleophiles to form stable condensation products[13].

Supported by National Natural Science Foundation of China (No.30770602) and Natural Science Foundation of Jiangsu Province, China (Nos. BK2010157 and BK2011167)

* Corresponding author. *E-mail address:* zhouxingqin@jsinm.org

Received date: 2013-04-08

^{99m}Tc-PQQ was previously prepared in our laboratory and found to potentially accumulate predominantly in the hippocampus and cortex, which have a high density of NMDAR[14]. However, ^{99m}Tc-PQQ is water-soluble and negatively charged and has chelating groups that further limit its ability to pass through the blood-brain barrier (BBB). Therefore, our research goal became to improve the structure of the ^{99m}Tc-PQQ to make it through the BBB. In this work, 4,5-dioxo-4,5-dihydro-1H-pyrrolo(2,3-f)quinoline-2,7, 9-tricarboxylic acid 2-ethyl ester 7,9-dimethyl ester (PQQE) (Fig.1) was synthesized on the basis of PQQ, labeled with ^{99m}Tc. Biological characteristics of ^{99m}Tc-PQQE including lipophilic and the charge properties were compared with that of ^{99m}Tc-PQQ. The biodistributions of ^{99m}Tc-PQQE in mice and brain regional distribution were studied. In addition, in vitro autoradiography assay was further performed.

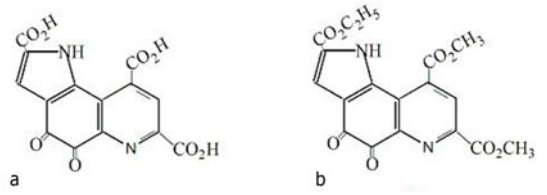

Fig.1 Chemical structures of PQQ(a) 4,5-dioxo- H-pyrrolo (2,3-f) quinoline-2,7,9-tricarboxylic acid and PQQE(b) 4,5-dioxo-4,5-dihydro-1H-pyrrolo (2,3-f) quinoline-2,7,9-tricarboxylic acid 2-ethyl ester 7,9-dimethyl ester.

2 Experimental section

2.1 Materials

The free ligand, PQQE, was synthesized in our lab. SnF_2, EDTA-2Na, Na_2HPO_4, KH_2PO_4 and other reagents were of analytical grade. Ebselen (EB) was purchased from Sigma-Aldrich (USA). Polyamide thin-film was from Taizhou Luqiao Sijia Bio-chemical Plastic Factory (China). ^{99m}Tc pertechnetate obtained from locally produced fission based ^{99}Mo/^{99m}Tc generator system was used for PQQE labeling.

2.2 Instruments

Wizard 1470 γ-automatic counting device (Perkin Elmer, USA), AC22105 and AC2105-type analytical balance (Sartorius, Germany), J2-HS Centrifuge (Beckman, USA), Quantitative bleeding vessel (Nantong Futura Medical Equipment Co., Ltd., China), C431200 Cyclone Storage Phosphor System (Perkin Elmer, USA), ^{99}Mo-^{99m}Tc generator (Chengdu Nuclear Isotope Qualcomm Inc., China) and Frozen section machine (Microtome-Cryostat MNT, Germany) were used in experiments. High performance liquid chromatography (HPLC) (600 system, Waters, USA) equipped with UV detector (2487, Waters, USA) and radiomatic 610TR detector (Perkin Elmer, USA) was also used.

2.3 Preparation of ^{99m}Tc-PQQE

PQQE was synthesized and characterized as previously reported in Ref.[15]. The purity of PQQE was assayed by HPLC. The content of PQQE was above 99.5%. ^{99m}Tc-PQQE was prepared using stannous fluoride (SnF_2) as reducing agent. 50 μl of EDTA-2Na (1 mg/mL) solution, 50 μL of SnF_2 solution (1 mg/mL, in 0.1 mol/L hydrochloric acid solution), 0.05 mL of PQQE (1 mg/mL) and 74 MBq $Na^{99m}TcO_4$ were added into a penicillin vial, then to which the phosphate buffer (pH 6.5) were added till the total volume reached 1mL. The reaction vial was left at boiling water for 30 min, then cooling to room temperature. Radiochemical purity of ^{99m}Tc-PQQE was tested by thin layer chromatography (TLC) and HPLC equipped with a gamma ray radiodetector and ultraviolet UV/Vis detector. ^{99m}Tc-PQQ was prepared as our previous experiments shown in Ref.[14].

2.4 Quality control of ^{99m}Tc-PQQE

2.4.1 TLC

The labeling yield of ^{99m}Tc-PQQE was assessed by TLC method using Polyamide thin-film as stationary phase while acetone: N-hexane: triethylamine (3:1:1) as the mobile phase.

2.4.2 HPLC

The Radiochemical (RCP) yield of ^{99m}Tc-PQQE was determined by a RHPLC performed on C18 column (Lichropher, C18, 4.6×250 mm, HanBang, China) using a flow rate of 0.8 mL·min^{-1} and UV detected at 249 nm (Fig.2). The solvent system consisted of 0.1% (v/v) trifluoroacetic acid (TFA) in acetonitrile (eluent A) and 0.1% (v/v) TFA in water (eluent B). The initial mobile phases composition was held at 5/95 (A/B) for 5 min followed by a linear gradient to 75/25 (A/B) from 5 to 20 min and then to 5/95 (A/B) from 20 to

25 min. The eluted radioactivity was monitored on line using a NaI probe and collected fractions were also measured by the gamma counter. Data were collected and processed with Waters Empower software.

2.4.3 Stability study

The stability of ^{99m}Tc-PQQE was studied at 25℃ for 6 h (Fig.3). The RCP of ^{99m}Tc-PQQE was determined by HPLC at various time points (0, 1, 2, 3, 4, 5, 6 h).

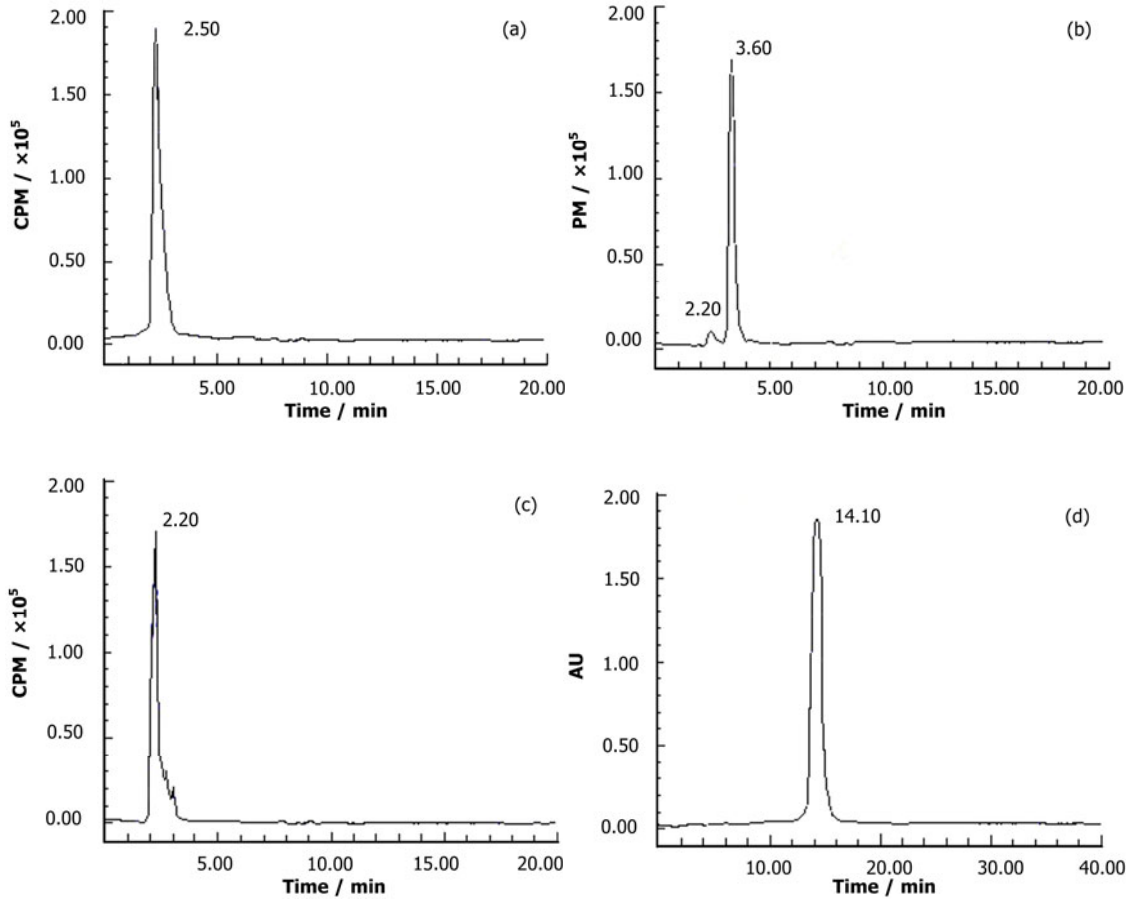

Fig.2 HPLC chromatograms of $^{99m}TcO_4^-$ (a), ^{99m}Tc-PQQE (b), ^{99m}Tc-colloid (c) and PQQE (d). (PQQE t_R = 14.1 min at UV detector λ=249 nm) (^{99m}Tc-PQQE t_R=3.6 min, ^{99m}Tc-colloid t_R=2.2 min and $[^{99m}TcO_4]^-$ t_R=2.5 min at Cd (Te) detector). (Lichropher, C18, 4.6×250 mm, 0.8 mL·min^{-1}, 249 nm. Eluent A: 0.1% TFA in acetonitrile, Eluent B: 0.1% TFA in water. 5/95 (A/B) for 5 min gradient to 75/25 (A/B) from 5 to 20 min and then to 5/95 (A/B) from 20 to 25 min.

2.5 Octanol/water partition coefficients and plasma protein binding

2.5.1 Octanol/water partition coefficient

The octanol/water partition coefficients were measured by the following procedure: 1 mL PBS (pH=7.4) saturated with 1-octanol and 1 mL 1-octanol saturated with PBS were added to a centrifuge tube containing 0.2 mL ^{99m}Tc-PQQE (0.37 MBq). The tube was capped and vigorously vortexed for 5 min at room temperature and then allowed to stand for 5 min. After reaching equilibrium, the tube was centrifuged at 2400 r/min for 10 min. Aliquots were taken from each phase and radioactivity counted. The partition coefficient was calculated by dividing the radioactivity of the 1-octanol layer with that of the water layer. The partition coefficient (log*P*) was calculated using the following equation:*P*=(activity in octanol−background activity)/(activity in aqueous layer−background activity). All experiments were performed in triplicate (Table 1).

The charge of ^{99m}Tc-PQQE was determined by paper electrophoresis according to the previous methods[14].

2.5.2 Plasma protein binding

A mixture of 0.1 mL of the ^{99m}Tc-PQQE (1.55 MBq, 0.16 MBq, 0.016 MBq) in 0.2 mL plasma was incubated for 3 h at 37°C. Following equilibrium, 1 mL 15% trichloroacetic acid was added to each tube, followed by vortexing and centrifuging at 2400 r/min

for 10 min. The supernatant was collected and the steps were repeated four times. The radioactivity of the supernatant and residue was counted using a gamma counter. Plasma protein binding was calculated by the relationship: plasma protein binding =[(residue counts)/(residue counts+supernatant counts)] ×100% (Table 1).

Table 1 Plasma protein binding and $P_{O/W}$ values of ^{99m}Tc-PQQ and ^{99m}Tc-PQQE

Test items		^{99m}Tc-memantine derivatives	
		^{99m}Tc-PQQ	^{99m}Tc-PQQE
Plasma protein binding (%)	High (1.55 MBq)	6.02	5.19
	Middle (0.16 MBq)	5.43	5.88
	Low (0.016MBq)	6.15	6.36
$P_{O/W}$ value		–1.46±0.16	0.72±0.11
Electric charge		negative electrode	neutral

2.6 Biodistribution in mice

The biodistribution of ^{99m}Tc-PQQE was studied in normal Kunming mice (20±2) g to evaluate pharmacokinetic properties. A volume of 0.2 mL of the purified radiotracer solution (~10 MBq) was injected into the mice via the tail vein. The mice (n=5) were sacrificed at 5, 15, 30, 60, 120, 180, 240, and 360 min after injection. Organs and brain regions of interest were dissected, weighed, and counted for radioactivity. The percentage of injected dose per gram (%ID/g) was calculated (Table 2，Table 4)[16].

Table 2 Biodistribution of ^{99m}Tc- PQQE in mice ($\bar{x}$±SD, n=5, %ID·g^{-1})

Regions	5 min	15 min	30 min	60 min	120 min	180 min	240 min	360 min
Heart	3.20±0.53	2.68±0.13	2.65±0.71	0.65±0.13	0.58±0.23	0.45±0.06	0.36±0.06	0.25±0.08
Liver	6.04±0.60	9.94±0.66	28.29±0.71	41.54±6.61	58.70±2.32	38.58±6.22	38.34±4.15	27.26±0.82
Spleen	3.76±0.47	3.66±0.57	3.30±0.34	2.67±0.14	2.48±0.39	2.17±0.26	1.52±0.08	1.42±0.28
Lung	8.95±0.46	6.11±0.81	5.00±0.42	2.26±0.92	1.88±0.47	1.46±0.23	1.62±0.63	0.65±0.19
Kidney	5.58±0.78	5.39±0.10	5.22±0.95	3.30±0.34	3.14±0.55	3.59±0.54	3.66±0.22	3.75±0.96
Stomach	35.71±2.52	33.44±1.57	30.35±1.44	27.07±1.42	20.95±1.22	19.40±4.72	14.36±1.87	6.39±1.73
Intestine	2.49±0.58	3.33±0.77	4.22±0.60	2.48±0.65	2.04±0.84	1.73±0.15	1.47±0.15	0.88±0.26
Gonads	1.62±0.39	2.03±0.16	2.17±0.59	0.83±0.28	0.85±0.75	0.47±0.29	0.32±0.18	0.13±0.01
Muscle	1.16±0.29	1.15±0.11	0.97±0.09	0.27±0.10	0.23±0.11	0.25±0.11	0.13±0.06	0.09±0.03
Skeleton	1.54±0.27	2.28±0.62	2.12±0.28	0.62±0.10	0.60±0.22	0.76±0.33	0.56±0.22	0.32±0.10
Blood	12.64±1.23	7.70±0.34	6.33±0.26	2.20±0.38	1.29±0.15	0.93±0.36	0.64±0.12	0.46±0.18
Brain	0.61±0.09	0.34±0.05	0.25±0.03	0.12±0.05	0.08±0.03	0.08±0.02	0.06±0.02	0.04±0.01

2.7 Blood kinetic tests

^{99m}Tc-PQQE (0.2 mL, 10 MBq) was injected through the tail vein into mice (20 g±2 g, n=5). At different times (2, 5, 10, 15, 30, 60, 120, 180, 240 and 360 min), 10 μl blood was taken from the tail vein by quantitative vessel bleeding. The samples were counted and the data were expressed as percentage of administered dose at each time interval (% ID·g^{-1}). The data were analyzed using 3p87 pharmacokinetic software to fit the appropriate compartment model.

2.8 *In vitro* autoradiography

Visualization of ^{99m}Tc-PQQE binding to NMDAR was performed by autoradiography of brain sections using storage phosphor images. The brains were excised and sliced to 20 μm horizontal sections from healthy Sprague-Dawley (SD) rat of (250±10) g. The slides were divided into two groups and operated as previously reported[14]. 0.01 mol/L EB was added to the slide in incubated solution as control group. The experimental group was pretreated with saline. The

phosphor plate was exposured for 60 min and scanned in the Cyclone Storage Phosphor System for approximately 30 min. The hippocampus and cortex were chosen as the interested sections where the NMDA receptor is abundant. The data were carried out using region of interest (ROI)-analysis and recorded as digital light intensity units (DLU) / mm^2, which were proportional to the radioactivity of the measured samples.

3 Results and discussion

3.1 Radiochemistry

^{99m}Tc-PQQE was characterized by HPLC (Fig.2). Under the selected chromatographic conditions, it was possible to separate the peaks corresponding to the complex ^{99m}Tc-PQQE (t_R=3.6 min) from ^{99m}Tc-colloid (t_R=2.2 min) and $[TcO_4]^-$ (t_R=2.5 min). In TLC test, $^{99m}TcO_4^-$ and ^{99m}Tc-PQQE moved towards the solvent front ($^{99m}TcO_4^-$, Rf=1.0; ^{99m}Tc-PQQE, Rf=0.6～0.7), while ^{99m}Tc-colloid remained at the point of spotting (Rf=0) in control group without PQQE.

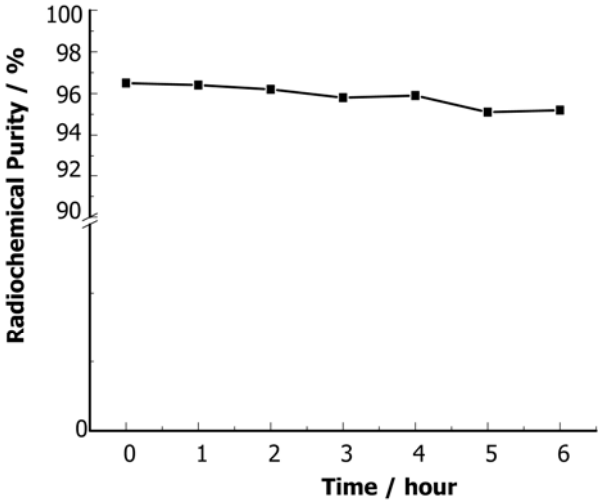

Fig.3 Stability of ^{99m}Tc-PQQE at room temperature *in vitro*.

3.2 Partition coefficients and plasma protein binding % (compared to ^{99m}Tc-PQQ)

One important factor that determines whether a drug penetrates the blood-brain barrier is its lipid-water partition coefficient. From Table 1, it can be seen that ^{99m}Tc-PQQE is lipophilic. However, ^{99m}Tc-PQQ is water-soluble. The electric charge and plasma protein binding were also listed in Table1.

3.3 Stability studies

The stability of the radiolabeled compound was also investigated over time. The radiochemical purity of ^{99m}Tc-PQQE was above 95% at room temperature for 6 hours (Fig. 3).

3.4 *In vivo* biodistribution

In vivo distribution of ^{99m}Tc-PQQE in mice is shown in Table 2. Stomach had a significantly greater uptake than all other tissues (p<0.05), followed by lung, and then by liver. The uptake of ^{99m}Tc-PQQE in liver significantly increased from 5 min to 120 min and decreased from 180 min to 360 min in the study. There was more ^{99m}Tc-PQQE uptake in liver than in kidney all the time. The major radioactivity may be metabolized by the hepatic other than renal system. The uptake of ^{99m}Tc-PQQE in brain was improved due to the ameliorating of charge and lipophilicity (Table 1). From Table 2, it can be seen that the uptake of ^{99m}Tc-PQQE in brain is 2.3 times of ^{99m}Tc-PQQ at 5 min[14].

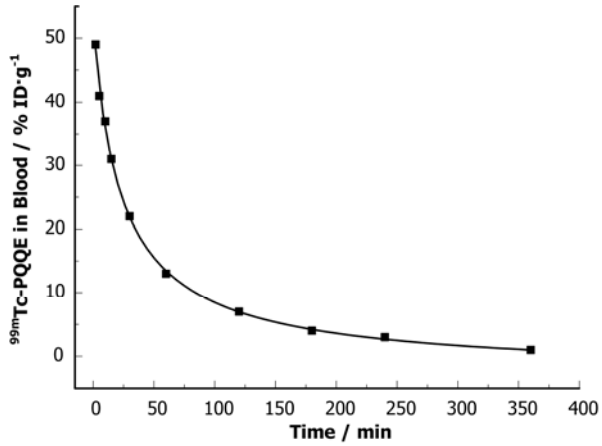

Fig.4 Blood kinetic curve of ^{99m}Tc-PQQE in mice

3.5 Blood kinetic studies

The compartment model of ^{99m}Tc-PQQE was a two-compartment model by the regression analysis. The blood kinetic curve was shown in the Fig.4. A dual-exponential equation, $Y=38.68e^{-0.027t}+7.25e^{-0.003t}$ was used. Here Y is %ID·g^{-1} in blood and t is the time after injection. The distribution-phase half-time ($t_{1/2\alpha}$) and elimination-phase half-time ($t_{1/2\beta}$) were calculated from the simulated dual-exponential curves. The pharmacokinetic parameters of ^{99m}Tc-PQQE were

summarized in Table 3. The $t_{1/2\alpha}$ results show that ^{99m}Tc-PQQ (18.16 min) slightly rapid distributed *in vivo* than ^{99m}Tc-PQQE (25.443 min). Moreover, the $t_{1/2\beta}$ results clearly indicate that the residence time of ^{99m}Tc-PQQE (203.916) in the body is twice as long as ^{99m}Tc-PQQ (100.45). The distribution of ^{99m}Tc-PQQ and ^{99m}Tc-PQQE *in vivo* are both quickly. However, the clearance of ^{99m}Tc-PQQ *in vivo* is much fast than ^{99m}Tc-PQQE. *In vivo* distribution of ^{99m}Tc-PQQE in mice indicate that the concentration ratio of drug to blood increase steadily over time.

Table 3 Pharmacokinetic parameters of ^{99m}Tc-PQQE in mice (6.66 MBq/0.2 mL, n=5)

Parameter	^{99m}Tc-PQQE	^{99m}Tc-PQQ
$t_{1/2a}$ / min	25.4	18.16
$t_{1/2\beta}$ / min	203.92	100.45
K_{12} / min^{-1}	0.011	0.013
K_{21}/ min^{-1}	0.007	0.017
K_e/ min^{-1}	0.013	0.016
AUC/ ID%g^{-1}min	3553.6	1040.78
CL/ mL·min^{-1}	0.028	0.096

Table 4 Biodistribution of ^{99m}Tc-PQQE in brain of mice ($\bar{x}$ ±SD, *n*=5, %ID·g^{-1})

Regions	5 min	15 min	30 min	60 min	120 min	180 min	240 min	360 min
Striatum	0.26±0.03	0.21±0.03	0.21±0.01	0.12±0.01	0.09±0.02	0.09±0.04	0.07±0.01	0.05±0.01
Hippocampus	0.51±0.01	0.39±0.02	0.26±0.01	0.22±0.01	0.20±0.03	0.16±0.02	0.12±0.01	0.09±0.02
Frontal lobe	0.45±0.04	0.39±0.03	0.30±0.04	0.18±0.02	0.17±0.04	0.14±0.02	0.12±0.02	0.11±0.01
Parietal lobe	0.35±0.03	0.39±0.03	0.26±0.05	0.15±0.02	0.09±0.01	0.10±0.02	0.09±0.01	0.06±0.01
Temporal lobe	0.23±0.02	0.22±0.01	0.18±0.04	0.08±0.02	0.06±0.01	0.08±0.03	0.06±0.00	0.06±0.02
Occipital lobe	0.29±0.02	0.21±0.02	0.16±0.03	0.11±0.02	0.08±0.01	0.08±0.01	0.08±0.03	0.06±0.01
Cerebellum	0.27±0.05	0.25±0.05	0.15±0.02	0.07±0.01	0.05±0.02	0.05±0.01	0.05±0.01	0.05±0.01
Thalamus	0.20±0.04	0.15±0.04	0.11±0.02	0.07±0.02	0.06±0.02	0.04±0.01	0.03±0.00	0.03±0.01
Hippocampus/Cerebellum	1.89	1.56	1.73	3.14	4.00	3.20	2.40	2.25
Frontal /Cerebellum	1.67	1.56	2.00	2.57	3.40	2.80	2.40	2.20

3.6 Brain regional distribution of ^{99m}Tc-PQQE

The brain regional distribution of ^{99m}Tc-PQQE was evaluated by measuring uptake in the region of interest including the striatum, hippocampus, thalamus, cerebellum, and cortex (frontal, occipital, parietal, and temporal lobes). The frontal lobe and hippocampus were used as the target regions since they have the highest density of NMDA receptors, and the cerebellum was used as a non-target region since it has the lowest density of NMDA. The brain regional distribution and the ratios of the target to nontarget counts for ^{99m}Tc-PQQE are showed in Table 4. The highest total regional brain uptake of ^{99m}Tc-PQQE was in the frontal lobe and hippocampus, where the NMDA receptor is very abundant. ^{99m}Tc-PQQE had a good target to nontarget ratio (hippocampus/ cerebellum) which preserved a higher value (peak 4.0 at 120 min) from 60 min to 180 min after injection. The ratio Frontal/cerebellum reached 3.4 at 120 min.

Significant abnormalities have been reported in the superior frontal gyrus in schizophrenia[17]. The prefrontal cortex was demonstrated to play a crucial role in modulating cognitive functions[18].

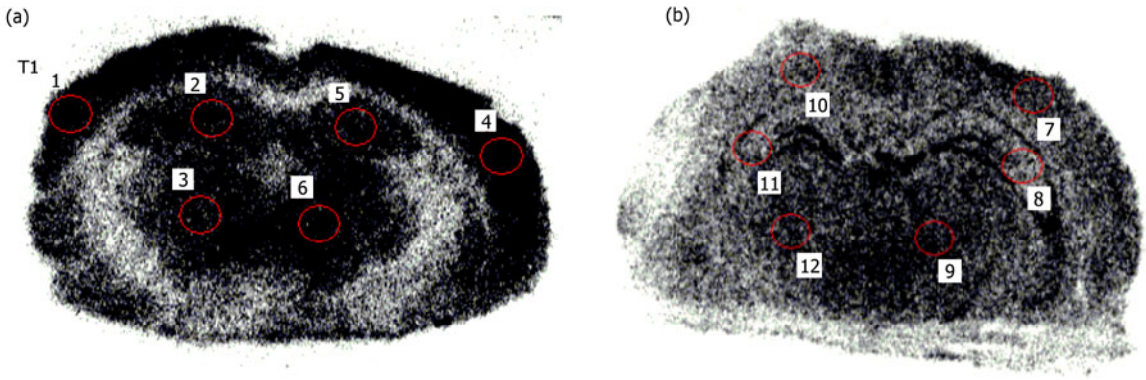

Fig.5 Autoradiography of ^{99m}Tc-PQQE in rat brain (Coronal plane) by storage phosphor imaging A: Brain section without pretreated B: Control section of EB-pretreated.

Table 5 DLU/mm^2 of ^{99m}Tc-PQQE in target regions

Regions	Experimental groups (Fig.5a)	EB-pretreated group (Fig.5b)
Cortex	289010.4	198137.1
Hippocampus	267094.7	161825.5
Thalamus	250263.2	228895.4
cortex/Thalamus	1.15	0.87
Hippocampus/Thalamus	1.07	0.71

3.7 *In vitro* autoradiography

The regional distribution of ^{99m}Tc-PQQE in rat brain was measured by autoradiograms (Fig.5). The cortex and hippocampus were chosen as the brain area of interest, the thalamus was chosen as the reference region. Data were measured by ROI analysis on the obtained storage phosphor images and were presented for the experimental, EB-pretreated group. Obviously, the uptake of ^{99m}Tc-PQQE in the cortex on experiment group was higher than EB-pretreated group in the cortex.

The ratios of hippocampus/thalamus were calculated in Table 5. As has been shown, the accumulation of ^{99m}Tc-PQQE in several brain regions, such as the hippocampus and cortex (areas known to have a high density of NMDAR), can be inhibited by EB.

4 Conclusion

^{99m}Tc-PQQ was prepared and the binding between ^{99m}Tc-PQQ and NMDAR *in vitro* and *in vivo* was characterized[14]. However, ^{99m}Tc-PQQ is water soluble and negatively charged and has chelating groups that limit its amounts into brain. To resolve this problem, opening the BBB by mannitol was used to enable ^{99m}Tc-PQQ to enter into the brain[19].

Furthermore, ^{99m}Tc-PQQE was prepared to improve the lipophilic and the charge properties (Table 1). Here we characterized ^{99m}Tc-PQQE and mapped the regional distribution of ^{99m}Tc-PQQE in brain. It is clear that the uptake amounts of ^{99m}Tc-PQQE in brain were significantly higher than ^{99m}Tc-PQQ. The levels of ^{99m}Tc-PQQE in brain were 2.3 times of ^{99m}Tc-PQQ at 5 min. Target tissues with abundant NMDAR, such as the hippocampus and cortex, also increased uptake and retention of ^{99m}Tc-PQQE. Furthermore, The AUC of ^{99m}Tc-PQQ (1040) is much smaller than ^{99m}Tc-PQQE (3553). AUC is the area under the curve of plasma concentration to time. The extent of drug absorption is proportional to the AUC. This result suggests that ^{99m}Tc-PQQE can be easily uptake in tissue, thus contributing to high-quality imaging of the target tissue. Further studies are needed to apply ^{99m}Tc-PQQE for NMDA receptor imaging.

References

1 Caughey W S, Raymond L D, Horiuchi M, *et al.* Proc Natl Acad Sci USA, 1998, **95:** 12117–12122.

2 Caspi S, Halimi M, Yanai A, *et al.* J Biol Chem, 1998, **273:** 3484–3489.

3 Stites T E, Mitchell A E, Rucker R B. J Nutr, 2000, **130:** 719–727.

4 McIntire W S. Annu Rev Nutr, 1998, **18:** 145–177.

5 Davidson V L. Adv Protein Chem, 2001, 58: 95–140.

6 Anthony C. Antioxid Redox Sign, 2001, **3:**757–774.

7 Steinberg F M, Gershwin E, Rucker R B. J Nutr, 1994, **124:**744–53.

8 Urakami T, Sugamura K, Niki E. Biofactors, 1995, **5:** 75–81.

9 Porat Y, Abramowitz A, Gazit E. Chem Biol Drug Des, 2006, **67:** 27–37.

10 Zhang Y, Feustel P J, Kimelberg H K. Brain Res, 2006, **1094:** 200–206.

11 Rucker R, Chowanadisai W, Nakano M, [J]. Altern Med Rev, 2009, **14:** 268–277.

12 Naito Y, Kumazawa T, Kino L, Suzuki O. Life Sci, 1993, **52:** 1909–1915.

13 Zhang P, Xu Y P, Sun J X, *et al.* Free Radical Res, 2009, **43:** 224–233.

14 Kong Y Y, Zhou X Q, Cao G X, *et al.* J Radioanal Nucl Ch, 2011, **287**：93–101.

15 Martin V P. Helv Chim Acta, 1993, **76:**1667-1673.

16 Cao G X, Zhou X Q, Kong Y Y, *et al.* Nucl Sci Teth, 2013, **36:** 010303.

17 Katsel P, Davis K L, Gorman J M, *et al.* Schizophr Res, 2005, **77:** 241–252.

18 Benes F M. Brain Res Rev, 2000, **31:** 251–69.

19 Zhou XQ, Kong YY, Cao GX, *et al.* J Radioanal Nucl Ch, 2013, **295:** 335–343.